

# Thermoelectric Measurement of Multi-Walled Carbon Nanotube Bundles by Using Nano-Probes

Yi-Bin Gao<sup>1</sup>, Ye Wang<sup>1</sup>, Jun-Yi Wang<sup>1</sup>, Sheng-Yong Xu<sup>1,2,\*</sup>, Xian-Long Wei<sup>1,2</sup>,  
Ming-Sheng Wang<sup>1,2</sup>, Yan Li<sup>1,3</sup>, and Lian-Mao Peng<sup>1,2,\*</sup>

<sup>1</sup>Key Laboratory for the Physics and Chemistry of Nanodevices, Peking University, Beijing 100871, China

<sup>2</sup>Department of Electronics, Peking University, Beijing 100871, China

<sup>3</sup>School of Chemistry, Peking University, Beijing 100871, China

We report here a method for measurement of thermoelectric power of quasi-one dimensional nanomaterials with a simple platform, where individual nanomaterial is assembled with nano-probes in a scanning electron microscope. This approach allows repeated manipulation and thermoelectric measurement of the same loaded nanosample with adjustable number of individual nanotubes or nanowires. It also allows assembly of multiple samples on one measurement stage. For multi-walled carbon nanotube bundles, we have observed a weak trend that, when the number of individual tubes in a bundle varies from ten millions to around a hundred thousand, the thermoelectric power almost remains at around 10  $\mu\text{V/K}$ . When the tube number in the bundle is further reduced, the up-limit of the thermoelectric power gradually increases to a value near 20  $\mu\text{V/K}$ .

**Keywords:** Thermoelectric Properties, Low-Dimensional Thermoelectrics, Multi-Walled Carbon Nanotubes.

## 1. INTRODUCTION

The thermoelectric power (or thermopower),  $S$ , defined as  $S = \Delta V / \Delta T$  and also known as Seebeck coefficient, is a measure of the Seebeck effect. By the Seebeck effect, an electrical potential,  $\Delta V$ , can be established when the two ends of a conductor or semiconductor have a temperature difference  $\Delta T$ . In a microscopic view, the Seebeck electrical potential is resulted from diffusion of charge carriers in the sample due to a temperature gradient. In a metal or a degenerate semiconductor,  $S$  is related to the carrier density,  $n$ , by  $S = (8\pi k_B^2 / (3e\hbar^2))m^*T(\pi/3n)^{2/3}$ , where  $m^*$  is the effective mass of the charge carrier.<sup>1</sup> More generally, the  $S$  value of a material can be written as<sup>2</sup>

$$S = \frac{1}{eT} \frac{\int_0^\infty \sigma(E)(E - E_F)dE}{\int_0^\infty \sigma(E)dE} \quad (1)$$

where  $e$  and  $T$  are the electron charge and temperature, respectively,  $E_F$  is the Fermi level,  $\sigma(E)$  is the energy-dependent differential electrical conductivity that is mainly determined by the scattering mechanism and density of state (DOS). Equation (1) shows that  $S$  is also a measure of the asymmetry in electrical conductivity with respect to  $E_F$ . Therefore, measurement of the  $S$  values can provide

clues about the charge carrier density, DOS near the Fermi level, and insight into the electronic structure of conventional thermoelectrics, organic semiconductors and even molecular junctions.<sup>1–8</sup>

The thermoelectric power is also one of the four parameters that determine the dimensionless figure-of-merit,  $ZT$ , of a thermoelectric material by  $ZT = S^2\sigma T/\kappa$ , where  $\sigma$  and  $\kappa$  are electrical conductivity and thermal conductivity of the material, respectively, and  $T$  is the absolute temperature. The theoretically predicted high  $ZT$  value in low-dimensional thermoelectrics,<sup>4,9–14</sup> has been demonstrated in 2-dimensional (2D) superlattices with a  $ZT$  value of 2.4,<sup>15</sup> which is twice as large as those of the best bulk thermoelectric materials. It is predicted that one-dimensional (1D) materials such as nanowires and nanotubes may exhibit even higher  $ZT$  values due to size effects and surface effects, yet this have not been experimentally observed. The best room temperature  $ZT$  value reported in 1D nanomaterials, is measured around 0.5 at the room temperature<sup>16,17</sup> from Si nanowires, far from the theoretically predicted values.<sup>9,14</sup> Partially due to the difficulty in thermoelectric measurement of nanomaterials, only a small portion of the thermoelectric nanowires, nanobelts and nanotubes ever synthesized have been characterized for all the parameters of  $S$ ,  $\sigma$ ,  $\kappa$  and  $ZT$ .<sup>18–23</sup> Reliable  $S$  value of a nanomaterial that measured with a relatively

\*Authors to whom correspondence should be addressed.

simple method is helpful for searching for novel 1D thermoelectric materials with high  $ZT$ .

The thermoelectric power of single nanowire or nanotube has been measured with sophisticated devices that are fabricated with electron-beam lithography, thin film deposition and etching techniques,<sup>16, 17, 19, 21–23</sup> or, by technique of *in situ* scanning tunneling microscope (STM) techniques.<sup>5, 24, 25</sup> However, for the thermoelectric studies of novel nanomaterials, to date only a few groups are able to perform these complicated measurements. In this paper we demonstrate that the thermoelectric power of nanowires or nanotubes can be measured with a much simpler platform with reasonable measurement error. This has been realized with the help of commercial nano-probes installed in a scanning electron microscope, which allow us to repeat the procedure of changing the number of individual nanosamples loaded on the platform and perform thermoelectric measurements, until only a single nanotube or a nanowire is remained, therefore to obtain statistic information of the same nanomaterial. By using this measurement approach, we demonstrate that for multi-walled carbon nanotubes with an average diameter of thirty nanometers, their thermoelectric power increases from around  $10 \mu\text{V/K}$  to near  $20 \mu\text{V/K}$  when the tube number in the bundle decreases from the order of  $10^7$  to below ten.

## 2. EXPERIMENTAL DETAILS

As shown in Figure 1(A), the sample platform consists of two separated copper blocks, namely “Stage 1” and “Stage 2”, each having a volume of  $1.8 \text{ cm}^3$ . The copper blocks are fixed on a piece of glass slide, where two pieces of plastic rings are used as spacers to reduce thermal conductance between the copper block and glass slide (Fig. 1). Each copper stage is embedded with a Pt100 temperature sensor for accurate measurement of the temperatures,  $T_1$  and  $T_2$ , of Stages 1 and 2 respectively. During measurement, Stage 1 is externally heated or cooled, while Stage 2 is maintained at room temperature. This enables us to establish a temperature difference up to 80 K between the two stages. Since copper surface may be easily oxidized and a bulk surface may have huge roughness in the view of nanoscale, we have mechanically fixed several pairs of 25  $\mu\text{m}$ -diameter Au-wire to the copper stages as extension of the electrodes. Each pair of Au-wire has a gap in between, which can be adjusted to several microns to tens of microns, depending on the sample lengths. Several pairs of Au-wire electrodes can be mounted on a single sample stage, as shown in Figure 1(B). This enables us to start an experiment by mounting multiple nanosamples, measure them and then remove the assembled nano-samples individually with a sharp tungsten tip of a nano-probe system, and measure the rest samples again. This procedure can be repeated till only one nanosample is remained on one pair of Au-wires (Fig. 1(B)).

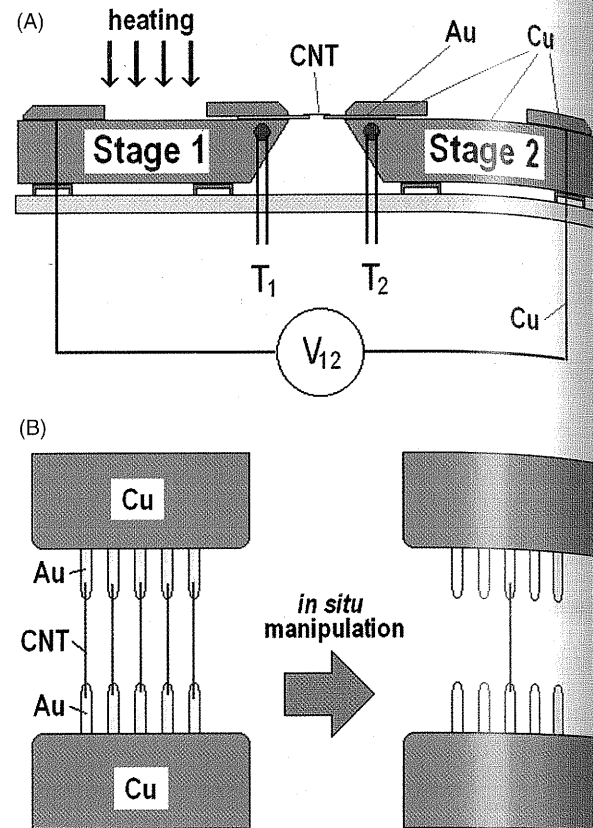


**Fig. 1.** (A) Schematic diagram of the measurement stage with two copper blocks, Stage 1 and 2, and a pair of 25- $\mu\text{m}$ -diameter Au-wires as the extension of electrodes. Two Pt100 temperature sensors are embedded close to the Au-wires. CNT samples are mounted between the pair of Au-wire electrode with a nanoprobe system in a SEM. (B) Schematic diagram of the central part of the testing stages, showing that several nanosamples (here 5 in the figure) can be assembled on the stages. After the first measurement, the loaded nanosamples can be partially removed *in situ* with a nanoprobe system for next thermoelectric measurement, and this procedure can be repeated several times until only one nanosample is remained on the stages.

The samples of multi-walled carbon nanotubes (MWCNTs) examined in this work are synthesized with a chemical vapor deposition (CVD) method using ferrocene as catalyst and cyclohexane as carbon source.<sup>26</sup> The lengths of these MWCNTs range from 2 to 3 mm. As revealed by scanning electron microscope (SEM) micrographs and transmission electron microscope (TEM) images, the MWCNTs in these samples have an average diameter of  $30 \pm 5 \text{ nm}$  (Fig. 2).

MWCNT bundle samples are assembled onto each pair of Au-wire electrodes with a nano-probe system (Kleindiek MM3A) installed in a field-emission SEM (FEI XL 30F). This nano-probe system has 4 tungsten (W) tips that can be moved up and down, backwards and forwards, with nanometer resolution in space. Therefore, they have been applied to manipulate individual nanowires and nanotubes for *in situ* characterization of their electrical transport, photo-electrical and mechanical properties.<sup>27–30</sup> The voltage difference,  $\Delta V = V_{12}$ , between two ends of a

Fig. 2.  
has been  
of indix  
(C) A h  
4 nm ai  
diamete

sample  
Au-wi  
meter.  
1 nV.)  
assem  
the tes

## 3. RE

Figure  
bled M  
MWC  
ules, t  
25  $\mu\text{m}$   
resista  
For  
thermo

where  
and  $\Delta V$   
in volta  
wrie sa  
 $0.17 \pm 0$   
age val  
the calc  
 $2 \times 10$   
of 2.00

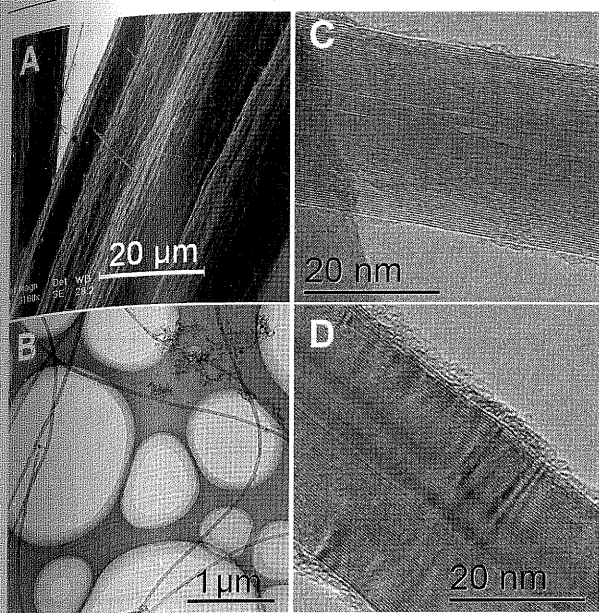


Fig. 2. (A) A SEM micrograph of a thick MWCNT bundle sample that has been measured in this work. (B) A low-magnification TEM images of individual MWCNTs, which have an average diameter of  $30 \pm 5$  nm. (C) A high resolution TEM image of MWCNT with an inner diameter of 4 nm and outer diameter of 27 nm. (D) A TEM image showing a 33 nm diameter MWCNT with lattice distortions.

sample that is assembled bridging Stages 1 and 2 through Au-wires, is measured with a Keithley 2182A nanovoltmeter. The resolution of voltage measurement is around 1 nV. For calibration, a 25  $\mu\text{m}$ -diameter Au-wire has been assembled directly connecting the two copper blocks as the testing sample.

### 3. RESULTS AND DISCUSSION

Figure 3 shows SEM micrographs of four assembled MWCNT bundle samples of varied diameters. The MWCNT samples exhibit extremely high Young's modulus, therefore they can be firmly wrapped around the 25  $\mu\text{m}$ -diameter Au-wire electrodes with a low contact resistance.<sup>31</sup>

For the testing sample of 25  $\mu\text{m}$ -diameter Au-wire, its thermoelectric power,  $S_{\text{Au}}$ , is calculated to be<sup>2</sup>

$$S_{\text{Au}} = S_{\text{Cu}} - \frac{\Delta V_{\text{Au}}}{\Delta T_{\text{Au}}} \quad (2)$$

where  $S_{\text{Cu}}$  is the Seebeck coefficient of the Cu stage,  $\Delta V_{\text{Au}}$  and  $\Delta T_{\text{Au}} \approx T_{12} = T_1 - T_2$  are the measured differences in voltage and temperature between two ends of the Au-wire sample, respectively. The measured  $\Delta V_{\text{Au}}/\Delta T_{\text{Au}}$  was  $0.17 \pm 0.02 \mu\text{V/K}$ , as shown in Figure 4, where the voltage values have been enlarged by a factor of 100. Here the calculated standard deviation of the fitted slope is only  $2 \times 10^{-4} \mu\text{V/K}$ . Since  $S_{\text{Cu}}$  is  $1.83 \mu\text{V/K}$ , we obtained  $S_{\text{Au}}$  of  $2.00 \pm 0.05 \mu\text{V/K}$ , which is consistent with the value of

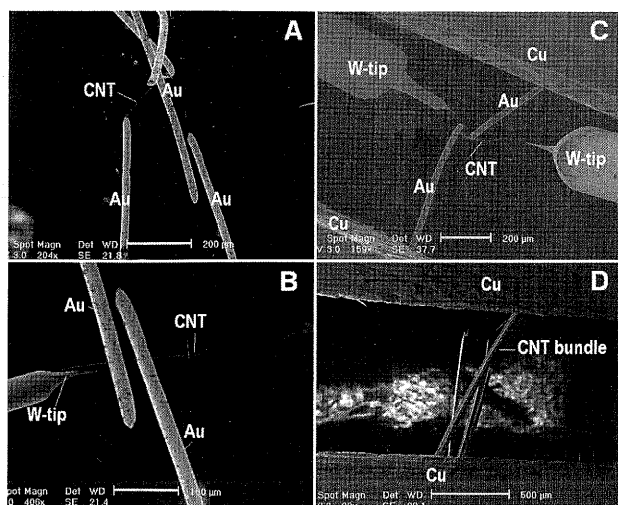


Fig. 3. SEM images of 4 assembled MWCNT bundle samples with different numbers of CNT tubes in each sample.

bulk Au,  $1.94 \mu\text{V/K}$ . Figure 4 shows that we have achieved a measurement error of around 3% for the very small  $S$  value of a 25-micron-diameter Au-wire over a temperature range of 300–315 K.

The MWCNT bundle samples were assembled between Stages 1 and 2 through Au-wires. We assumed the temperature difference in each piece of the Au-wire was negligible as compared to that in the bundle sample under test. The volumes of the copper block stages, Au-wires and the MWCNT bundle samples are of the order of  $10^3 \text{ mm}^3$ ,  $10^6 \mu\text{m}^3$ , and  $10^{-2} \mu\text{m}^3$ , respectively. Therefore the ratios among them are  $10^{14}:10^8:1$ . These huge ratios ensure that the temperature difference between the Au-wire and the copper stage, and between the nanosample and the Au-wire, are not large. We can take the temperature difference between two copper stages,  $\Delta T_{12} = T_1 - T_2$ , as the temperature difference between two ends of the assembled sample,

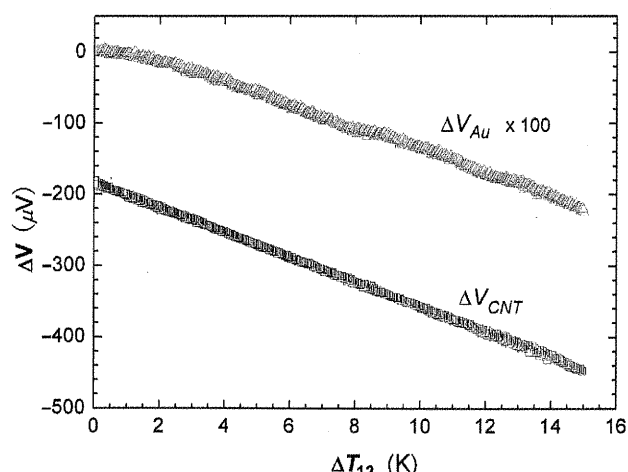


Fig. 4. Experimental  $\Delta V - \Delta T_{12}$  data that measurement from a 25- $\mu\text{m}$  diameter Au-wire and a MWCNT bundle sample with a tube number around 30.

$\Delta T_{\text{CNT}}$ . That is,  $\Delta T_{\text{CNT}} \approx \Delta T_{12}$ . And, considering the Ohmic contact between the Au-wire and copper block, and MWCNTs are all metallic,<sup>32</sup> we have  $\Delta V_{\text{CNT}} \approx \Delta V$ . Thus the  $S$  value of a MWCNT bundle,  $S_{\text{CNT}}$ , can be calculated by

$$S_{\text{CNT}} \cong S_{\text{Cu}} - \frac{\Delta V_{\text{CNT}}}{\Delta T_{\text{CNT}}} \quad (3)$$

where  $S_{\text{Cu}}$  is the thermoelectric power of the Cu stage,  $\Delta V_{\text{CNT}}$  and  $\Delta T_{\text{CNT}}$  are the voltage and temperature differences between two ends of the assembled MWCNT bundle, respectively. Figure 4 plots one set of original measurement data  $\Delta V - \Delta T_{12}$  of one MWCNT bundle sample. The slope is calculated to be  $-17.39 \mu\text{V/K}$ . By using Eq. (3), the  $S$  value of the MWCNT sample is thus determined to be  $19.2 \pm 0.5 \mu\text{V/K}$ . To reduce the possible temperature gradient in the Au-wire, one can further improve the platform by reducing the length of the Au-wire electrodes extending out of the copper blocks to a few microns.

The error in voltage measurements was less than  $0.1 \mu\text{V}$  over a signal range of  $10$ – $100 \mu\text{V}$  (see Fig. 4), which leads to an upper limit of  $0.1$ – $1\%$ . For the error in temperature measurement, we define  $t_1$  as the temperature difference between the measured data of Stage 1 and that of one end of the MWCNT bundle connecting to the stage. Similarly, we define  $t_2$  for the Stage 2 side. Briefly  $t_1$  and  $t_2$  should be functions of the absolute temperature and contact situation (e.g., the thermal contact resistance) at the sample-electrode regions. The absolute error in measurement of the temperature difference between two ends of the assembled sample is then  $t \equiv t_1 + t_2$  (or  $t_1 - t_2$ , depending on the signs). In our measurements, the temperature of Stage 1,  $T_1$ , is increased from  $\sim 300 \text{ K}$  to  $310$ – $380 \text{ K}$ , while the temperature of Stage 2,  $T_2$ , is kept at  $\sim 300 \text{ K}$ . Assuming the contact is stable and the thermal contact resistance remains the same, we expect that the values of  $t_1$  and  $t_2$  do not change remarkably within this temperature region. And, the thermoelectric power  $S$  is calculated from the slope of  $\Delta V - \Delta T_{12}$  curve, as shown in the Eqs. (2) and (3) and Figure 4. Therefore, constant  $t_1$  and  $t_2$  (thus  $t$ ) will lead only to a horizontal shift of the measured  $\Delta V - \Delta T_{12}$  curve, and this will not affect much the calculated value of  $S$ . Thus the measurement error in  $S$  values is determined rather by the relative change of  $t_1$  and  $t_2$  in the measurement procedure.

Another factor that may cause extra error or even failure in thermoelectric measurement of a nanomaterial is the electrical contact between the sample and the Au-wire electrodes. When the contact resistance is much smaller than the input impedance (about  $10 \text{ G}\Omega$ ) of Keithley 2182A Nanovoltmeter used in our measurements, the contact resistance does not affect the voltage measurement across the sample. For MWCNT bundle samples, we can apply a suitable excitation current to reduce the contact resistance by 1–2 orders of magnitude from the original setup. Figure 5(A) shows SEM images of a thin MWCNT

bundle loaded on a pair of Au-wire electrodes. The *in situ* voltage–current measurement data (Fig. 5(B)) of nominal electrical resistances measured from the three different runs, defined as  $R = V/I$ , are  $6.73$ ,  $0.632$ , and  $0.361 \text{ M}\Omega$ , respectively. This resistance consists of contact resistance at the MWCNT-bundle/Au-wire region, the resistances of the MWCNT bundle, Au-wire, copper block and measurement cables. The linear  $V-I$  curve of the third run in Figure 5 clearly shows that Ohmic contact has been established between MWCNT and Au wire, and no electrical potential exists at the contact region. The measured

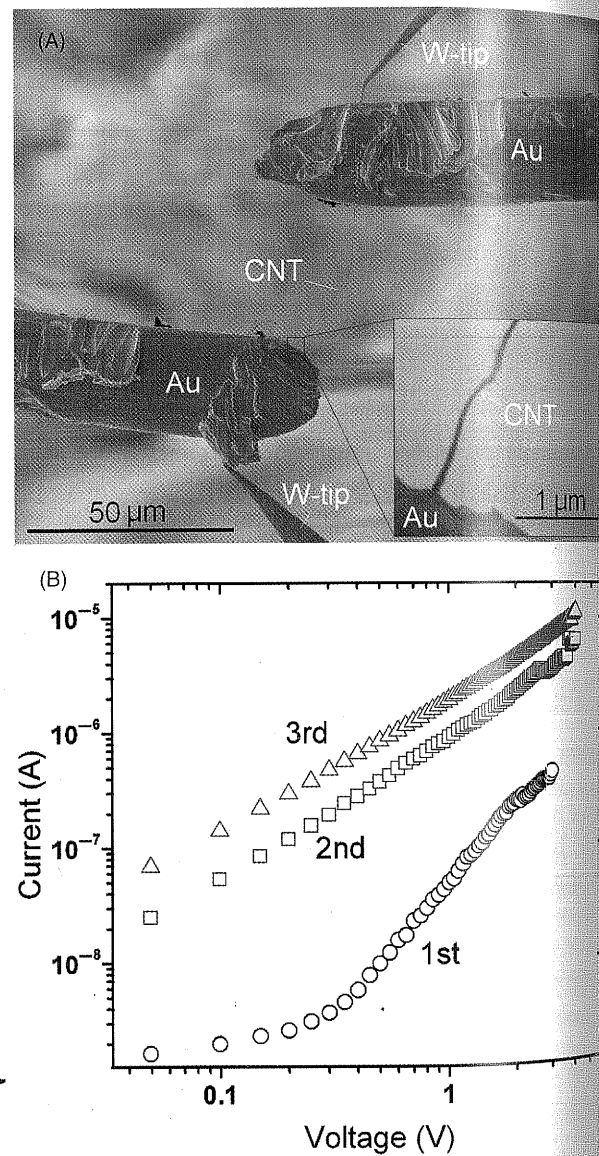


**Fig. 5.** (A) A SEM image of a thin MWCNT bundle loaded on a pair of Au-wire electrodes by using two W-tips. The inset is an enlarged SEM image of one end of the bundle sample that connects to the Au-wire electrode. (B) *In situ* measurement data of  $V-I$  of the loaded bundle sample, where after applying an excitation current to the loaded sample for minutes, the measured resistance of the third run is ten times smaller than that of the first run, and Ohmic contact of the MWCNT bundle to the Au-wire electrodes has been achieved.



ded on a pair  
enlarged SEM  
the Au-wire  
oaded bundle  
oaded sample  
times smaller  
NT bundle to

nominal resistivity of  $2.8 \times 10^{-3}$  Ω-cm is consistent with previously reported data of CVD-made MWCNTs.<sup>33</sup>

The remarkable decreases of the total resistance in the second and third runs are mainly resulted from decrease of the contact resistance at the MWCNT-bundle/Au-wire region. This is achieved by applying an electrical current of proper intensity that causes Joule heating at these contact regions, which removes surface impurities such as oxides, water or gas molecules by enhanced diffusion and/or vaporization. CNT has a very high melting point therefore remains undamaged. We have shown that, by applying a current with suitable intensity, one can also establish good electrical contact between a W-tip and single-walled CNT,<sup>34</sup> between a W-tip and a ZnO rod or SnO<sub>2</sub> nanoparticle,<sup>35</sup> or eliminate the amorphous carbon deposition on the CNT surface.<sup>36</sup> Electrical Joule heating can also be used to remove surface oxide layer of a W-tip,<sup>37</sup> as W has also a very high melting point.

However, we have noted that if the surface layer of impurity or oxide of a nanomaterial was too thick that no electrical current could be passed through, then the Joule heating method failed. In such cases the electrical contact resistance was comparable to or larger than the input impedance of the voltmeter, therefore we could not measure the voltage signals and obtain the thermoelectric power value of the sample.

Considering the complexity and uncertainty of thermal and electrical contact between MWCNT bundles and Au-wire, we estimated that the measurement error in thermoelectric power values was at the order of 10%, good enough for a qualitative analysis.

One remarkable advantage of our measurement method is the feasibility of modifying assembled samples *in situ* for repeated measurements of the same nanomaterial before and after the modification. Figure 6 shows *in situ* manipulation of a MWCNT bundle sample with a W-tip. The originally assembled MWCNT bundle sample consisted of roughly 500 nanotubes, and its thermoelectric power was measured to be  $16.0 \pm 0.5 \mu\text{V/K}$ . Then the sample was put back to the SEM and the major part of the bundle was removed with a W-tip (Figs. 6(A) and B)). The remaining sample (Fig. 6(C)) consisted of only around  $30 \pm 10$  nanotubes, with a thermoelectric power of  $19.4 \pm 0.5 \mu\text{V/K}$ . For very thick bundles, we have assembled the samples by fixing them directly under two pieces of copper plates on Stages 1 and 2, respectively, as shown in Figure 3(D).

For the same bunch of MWCNT samples grown on one piece of silicon substrate, we have measured bundles samples that consist of varied number of individual tubes,  $N$ , from the order of 10 to  $10^7$ . The number of tubes in each bundle is estimated based on its diameter measured in SEM micrograph, by taking the average diameter of a MWCNT tube as  $30 \pm 5 \text{ nm}$  (Fig. 2). The  $S$  values of these samples range from around  $10 \mu\text{V/K}$  to  $20 \mu\text{V/K}$ , as

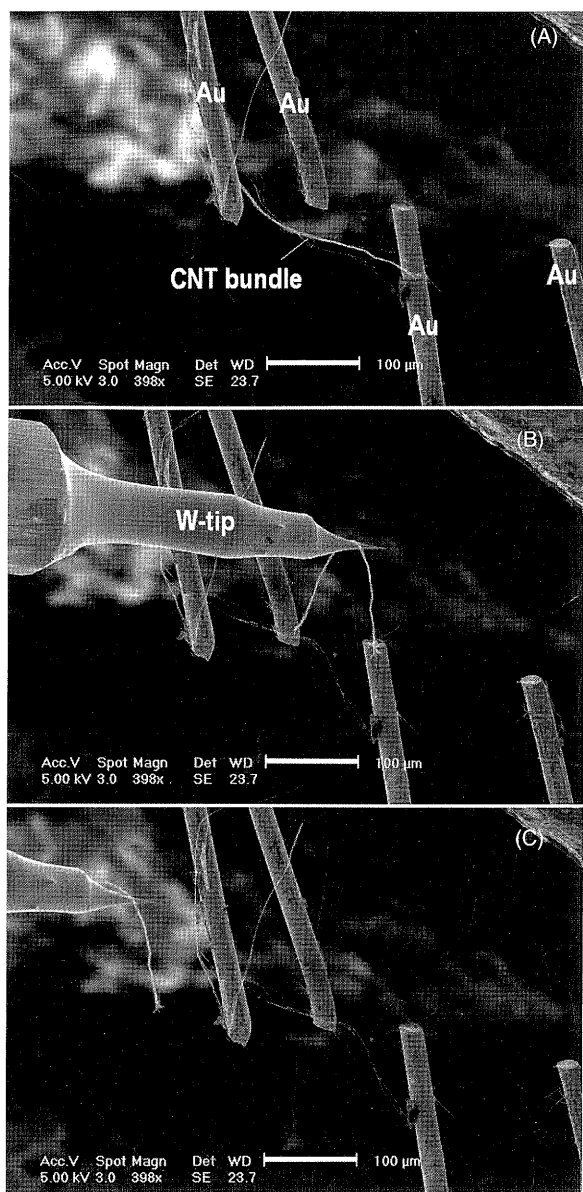


Fig. 6. SEM images show *in situ* manipulation of a MWCNT bundle sample with a W-tip. (A) A MWCNT bundle sample assembled between a pair of 25-micron diameter Au-wires. (B) The major part of the MWCNT bundle is removed with a W-tip in a SEM. (C) A remaining thin bundle of around 30 nanotubes of MWCNT between the two Au-wire electrodes. The scale bar is 100 micron.

shown in Figure 7. The scatter can be naturally understood in the way that the thermoelectric power of MWCNTs is sample dependent. Several factors can affect the measured data, among which are the differences in defect density, adsorption of gas molecules and impurity level. Figure 7 reveals a weak trend that thinner bundles have higher  $S$  values. Roughly the up-limit of  $S$  value decreases with increasing number of tubes in the sample, from near  $20 \mu\text{V/K}$  at  $N$  of the order of 10, to near  $10 \mu\text{V/K}$  at  $N \approx 10^5$ , then maintains at the level around  $10 \mu\text{V/K}$  till  $N \approx 10^7$ .

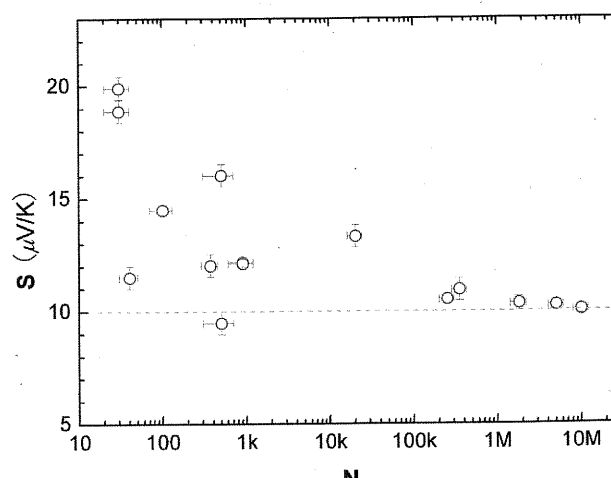


Fig. 7. The measured thermoelectric powers of MWCNT bundle samples with varied number of individual tubes from  $10^7$  to around 30. The value of  $10 \mu\text{V/K}$  is indicated with a dash line.

The dependence of  $S$  value on the number of tubes in the bundle can be understood with the effect of oxygen adsorption on the tube surface.<sup>38-40</sup> Jin et al.<sup>38</sup> reported a detailed study on CVD-made MWCNT bundles. After 4 MWCNT bundle samples from the same bunch were not annealed, annealed at 100, 1250 and 2800 °C in Ar for 4 hours, their  $S$  values at 300 K were measured to be 15, 13, 8 and  $-30 \mu\text{V/K}$ , respectively, and each sample showed different temperature dependence of their electrical and thermoelectrical properties. For single-walled CNTs (SWCNTs), Collins et al.<sup>39</sup> found that their  $S$  values at 350 K were very sensitive to the ambient gas, and could switch from positive  $20 \mu\text{V/K}$  in ambient oxygen environment to  $-10 \mu\text{V/K}$  in vacuum. Bradley et al.<sup>40</sup> showed similar results, that the  $S$  values of SWCNTs at 300 K could decrease sharply from a positive value of 15 to  $40 \mu\text{V/K}$  in ambient oxygen environment to a negative value of  $-20$  to  $-60 \mu\text{V/K}$  when the samples were put in ultrahigh vacuum environment. This has been attributed to removal of adsorbed oxygen from the tube surface. The MWCNTs used in our experiments were exposed to air, therefore had been presumably adsorbed with oxygen. The most available sites of a MWCNT bundle for oxygen adsorption are the outmost layer of tubes and some interstitial spaces between the tubes. For tubes at the inner part of the bundle, the outer layers of tubes serve as the barrier for diffusion of oxygen molecules, thus should be less adsorbed with oxygen. Our experimental results imply that, for a bundle having less than  $10^3$  individual MWCNTs, the oxygen adsorption effect on  $S$  value becomes dominant. This trend is consistent with previously reported  $S$  values of carbon nanotube samples in forms of individual tubes, thick bundles, and thin films.<sup>38-41</sup>

Our measurement stages cannot sustain a high annealing temperature. We have measured several samples in

vacuum for hours with the sample stages being heated to 400 K. However, no remarkable change in the thermoelectric power was observed. Annealing at this relatively low temperature seems not sufficient to remove the adsorbed gasses or other impurities in the samples.

#### 4. CONCLUSION

We have demonstrated here a flexible method for thermoelectric measurement of quasi-one dimensional nanomaterials, where the number of samples and the number of individual nanotubes (or nanowires) in the same assembled sample can be adjusted *in situ* for statistic analysis. For MWCNT bundles, we have observed a weak trend that, the up-limit of thermoelectric power of the samples remains at around  $10 \mu\text{V/K}$  when the bundle consists of more than  $10^4$  to  $10^7$  tubes, but gradually increases to values near  $20 \mu\text{V/K}$  when the tube number in the bundle is reduced to the order of ten. We suggest that this may be attributed to the surface effects, e.g., the surface adsorption of oxygen on the thermoelectric power of the bundles.

**Acknowledgment:** We acknowledge financial support from National Science Foundation of China (Grant No. 10774002), and Ministry of Science and Technology of China (Grant No. 2006CB932401).

#### References and Notes

1. G. J. Snyder and E. S. Toberer, *Nat. Mater.* 7, 105 (2008).
2. P. Reddy, S. Y. Jang, R. A. Segalman, and A. Majumdar, *Science* 315, 1568 (2007).
3. J. Heremans, V. Jovovic, E. S. Toberer, A. Saramat, K. Kurosaki, A. Charoenphakdee, S. Yamanaka, and G. J. Snyder, *Science* 321, 554 (2008).
4. L. D. Hicks and M. S. Dresselhaus, *Phys. Rev. B* 47, 12727 (1993).
5. H. K. Lyeo, A. A. Khajetoorians, L. Shi, K. P. Pipe, R. J. Ram, A. Shakouri, and C. K. Shih, *Science* 303, 816 (2004).
6. B. Poudel, Q. Hao, Y. Ma, Y. Lan, A. Minnich, B. Yu, X. Yan, D. Wang, A. Muto, D. Vashaee, X. Chen, J. Liu, M. S. Dresselhaus, G. Chen, and Z. F. Ren, *Science* 320, 634 (2008).
7. K. P. Pernstich, B. Rössner, and B. Batlogg, *Nat. Mater.* 7, 321 (2008).
8. J. Baheti, J. A. Malen, P. Doak, P. Reddy, S. Y. Jang, T. Don Tilley, A. Majumdar, and R. A. Segalman, *Nano Lett.* 8, 715 (2008).
9. L. D. Hicks, T. C. Harman, X. Sun, and M. S. Dresselhaus, *Phys. Rev. B* 53, R10493 (1996).
10. E. N. Bogacheck, A. G. Scherbakov, and U. Landman, *Phys. Rev. B* 60, 11678 (1999).
11. A. Majumdar, *Science* 303, 777 (2004).
12. M. S. Dresselhaus, G. Chen, M. Y. Tang, R. G. Yang, H. Y. Lee, D. Z. Wang, Z. F. Ren, J. P. Fleurial, and P. Gogna, *Adv. Mater.* 18, 634 (2007).
13. W. C. Kim, R. Wang, and A. Majumdar, *Nanotoday* 2, 40 (2007).
14. T. T. M. Vo, A. J. Williamson, V. Lordi, and G. Galli, *Nano Lett.* 8, 1111 (2008).
15. R. Venkatasubramanian, E. Siivola, T. Colpitts, and B. O'Quinn, *Nature* 413, 597 (2001).

heated to  
ermoelec-  
tively low  
adsorbed

or thermo-  
nanoma-  
number of  
assembled  
lysis. For  
that, the  
s remains  
more than  
values near  
reduced to  
tributed to  
of oxygen

al support  
Grant No.  
nology of

08).  
ndar, *Science*

K. Kurosaki,  
*Science* 321,

3 47, 12727

, R. J. Ram,

Yu, X. Yan,  
Dresselhaus,

*Later. 7, 321*

Don Tiley,  
(2008).

Dresselhaus, *Phys.*

*Phys. Rev. B*

3, H. Y. Lee,  
*Adv. Mater.* 38,

40 (2007).  
*Nano Lett.* 8,

B. O'Quinn,

4991, 2010

*J. Nanosci. Nanotechnol.* 10, 4985–4991, 2010

16. A. I. Boukai, Y. Bunimovich, J. Tahir-Kheli, J. K. Yu, W. A. Goddard III, and J. R. Heath, *Nature* 451, 168 (2008).
17. A. I. Hochbaum, R. K. Chen, P. D. Delgado, W. J. Liang, E. C. Garnett, M. Najarian, A. Majumdar, and P. D. Yang, *Nature* 451, 163 (2008).
18. J. Heremans and C. M. Thrush, *Phys. Rev. B* 59, 12579 (1999).
19. P. Kim, L. Shi, A. Majumdar, and P. L. McEuen, *Phys. Rev. Lett.* 87, 25502 (2001).
20. J. P. Heremans, C. M. Thrush, D. T. Morelli, and M. C. Wu, *Phys. Rev. Lett.* 88, 216801 (2002).
21. L. Shi, D. Y. Li, C. H. Yu, W. Y. Jang, D. Y. Kim, Z. Yao, P. Kim, and A. Majumdar, *J. Heat Transf.* 125, 881 (2003).
22. C. H. Yu, L. Shi, Z. Yao, D. Y. Li, and A. Majumdar, *Nano Lett.* 5, 1842 (2005).
23. A. Boukai, K. Xu, and J. R. Heath, *Adv. Mater.* 18, 864 (2006).
24. Z. X. Bian, A. Shakouri, L. Shi, H. K. Lyeo, and C. K. Shih, *Appl. Phys. Lett.* 87, 053115 (2005).
25. C. Dames, S. Chen, C. T. Harris, J. Y. Huang, Z. F. Ren, M. S. Dresselhaus, and G. Chen, *Rev. Sci. Instrum.* 78, 104903 (2007).
26. X. T. Zhang, J. Zhang, R. M. Wang, and Z. F. Liu, *Carbon* 42, 1455 (2004).
27. Q. Chen, S. Wang, and L. M. Peng, *Nanotechnol.* 17, 1087 (2006).
28. L. Shi, Y. M. Xu, S. K. Hark, Y. Liu, S. Wang, L. M. Peng, K. Wang, and Q. Li, *Nano Lett.* 7, 3559 (2007).
29. X. L. Wei, Q. Chen, Y. Liu, and L. M. Peng, *Nanotechnol.* 18, 185503 (2007).
30. M. Gao, W. L. Li, Y. Liu, Q. Li, Q. Chen, and L. M. Peng, *Appl. Phys. Lett.* 92, 113112 (2008).
31. X. L. Wei, Y. Liu, Q. Chen, M. S. Wang, and L. M. Peng, *Adv. Funct. Mater.* 18, 1555 (2007).
32. J. C. Charlier, X. Blase, and S. Roche, *Rev. Mod. Phys.* 79, 677 (2007).
33. R. Z. Ma, C. L. Xu, B. Q. Wei, J. Liang, D. H. Wu, and D. J. Li, *Mater. Res. Bullet.* 34, 741 (1999).
34. X. L. Wei, Q. Chen, S. Y. Xu, L. M. Peng, and J. M. Zuo, *Adv. Funct. Mater.* 19, 1753 (2009).
35. L. Shi, Y. M. Xu, S. K. Hark, Y. Liu, S. Wang, L. M. Peng, K. W. Wong, and Q. Li, *Nano Lett.* 7, 3559 (2007).
36. X. L. Wei, Y. Liu, Q. Chen, and L. M. Peng, *Nanotechnol.* 19, 355304 (2008).
37. J. Shen, W. Wang, Q. Chen, M. S. Wang, S. Y. Xu, Y. L. Zhou, and X. X. Zhang, *Nanotechnol.* 20, 245307 (2009).
38. R. Jin, Z. X. Zhou, D. Mandrus, I. N. Ivanov, G. Eres, J. Y. Howe, A. A. Puretzky, and D. B. Geohegan, *Physica B* 388, 326 (2007).
39. P. G. Collins, K. Bradley, M. Ishigami, and A. Zettl, *Science* 287, 1801 (2000).
40. K. Bradley, S. H. Jhi, P. G. Collins, J. Hone, M. L. Cohen, S. G. Louie, and A. Zettl, *Phys. Rev. Lett.* 85, 4361 (2000).
41. M. L. Tian, F. Q. Li, L. Chen, Z. Q. Mao, and Y. H. Zhang, *Phys. Rev. B* 58, 1166 (1998).

Received: 4 August 2009. Accepted: 8 September 2009.